# Interference Alleviation for Asynchronous Multigateway Multibeam Precoding

Huda Ali*, Qing Su*, Wenguan Zhang*,§, Zihao Wang†, Mohammed A. M. Ali* and Rui Chen*,§
*State Key Lab. of ISN, Xidian University, Xian, China
§Guangzhou Institute of Technology, Xidian University, Guangzhou 510700, China
†School of Electronics and Computer Science, University of Southampton, Southampton, United Kindom

***Abstract*—To enhance spectral efficiency, multigateway multibeam satellite systems with full frequency reuse have been developed, where each gateway serves a cluster of beams. While precoding is essential for mitigating intra- and inter-cluster interference, most studies assume synchronous reception, a condition rarely met due to gateway separation, which introduces differential propagation delays and results in asynchronous reception. This paper investigates asynchronous multigateway multibeam satellite systems, studying how both natural and intentional timing offsets can improve system performance. Specifically, we analyze a natural asynchrony model arising from gateway spacing. To further exploit asynchrony, we propose an intentional asynchrony model that introduces deliberate timing offsets at the satellite for each user. A weighted minimum-mean-square-error (WMMSE) precoder is then employed to mitigate the resulting interference. Simulation results show that the proposed approach achieves significant throughput gains, outperforming a conventional precoding technique designed for synchronous transmission.**

***Index Terms*—Multibeam satellite systems, multigateway architecture, asynchronous transmission, weighted MMSE.**

## I. Introduction

Satellite communication is essential for providing internet and services to remote and rural areas lacking terrestrial infrastructure [1]. To meet rising demands for fast and reliable connectivity, modern systems use multibeam architectures with multiple ground gateways, each serving a cluster of beams [2]. These systems employ full frequency reuse across beams to improve spectral efficiency (SE) but this introduces interference among beams within the same cluster (intra-cluster interference) and among beams across different clusters (inter-cluster interference), reducing system performance [3]. To address this, precoding is applied at the transmitter.

Many precoding techniques have been developed to reduce interference; however, most studies assume synchronous signal arrival. In practice, varying gateway-user distances introduce differential propagation delays, leading to asynchronous reception, where both desired and interfering signals arrive at different times. Even if gateways transmit simultaneously.

Despite its practical importance, asynchronous transmission in multigateway satellite systems remains underexplored, with most existing studies focusing on perfect synchronization [4]–[6]. In particular, the authors in [4] studied multigateway multibeam precoding, addressed feeder link interference, limited gateway cooperation, and imperfect channel state information (CSI), and adapted it for multicast scenarios. Reference [5], [7] proposed multigateway precoding in the presence of feeder link interference under sum power constraints, using a two-stage interference mitigation method and an iterative optimization method, respectively. Finally, [6] proposed a multigateway architecture based on recursive hybrid precoding to compress feeder link bandwidth and decomposed the optimization problem to improve SE through the co-design of satellite-terrestrial precoding.

Several studies showed that time asynchrony can provide notable performance benefits [8]–[10]. Specifically, [8] showed that interference between cooperating base stations remained asynchronous despite timing-advance, and proposed precoding methods to improve downlink performance. Furthermore, [9] derived closed-form expressions for asynchronous interference in MIMO broadcast channels. Reference [10] proposed a cooperative beamforming scheme for multiple low earth orbit (LEO) satellite systems that leveraged time asynchrony to improve sum rate under coherent transmission.

To the best of authors' knowledge, no existing research addresses asynchronous transmission in multigateway multibeam satellite systems, despite its promising advantages. This paper studies asynchronous transmission system that accounts for natural time delays arising from the geographical separation of gateways. These delays cause asynchronous reception of inter-cluster interference, which can be exploited to reduce its power. To further leverage asynchrony, the system is extended by intentionally introducing timing offsets at the satellite for each user, allowing mitigation of both intra- and inter-cluster interference and improving overall performance. The weighted minimum-mean-square-error (WMMSE) precoding algorithm is then applied to suppress interference, allowing more accurate modeling and achieving superior performance compared to conventional method that assume perfect synchronization.

## II. System Model

We consider the forward link of a multigateway multibeam satellite system, where a geostationary earth orbit (GEO) satellite provides wide area coverage and serves a large number of users. To enhance SE, full frequency reuse is applied across all beams. Let $\mathcal{L} = \{1, 2, \ldots, L\}$ represent the set of $L$ gateways, where each gateway $l \in \mathcal{L}$ serves a cluster of $B$ beams, indexed by $\mathcal{B} = \{1, 2, \ldots, B\}$, as shown in Fig. 1. Under the single feed per beam architecture, each gateway uses $B$ satellite feeds, one per beam, so the feed index matches the

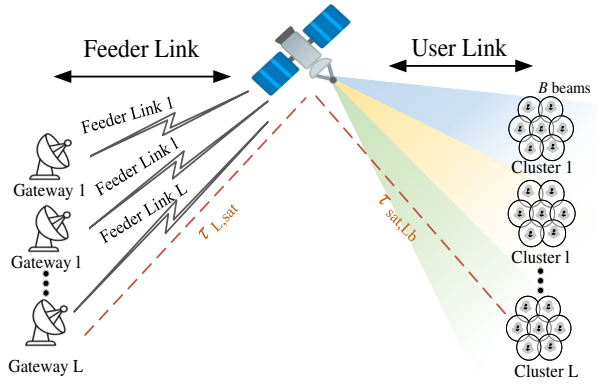


Fig. 1. Multigateway Multibeam satellite communication system model.

beam index. We assume one active user per beam, each with a single receive antenna, perfect CSI, and full knowledge of propagation delays.

### A. Signal Model

Let $M$ denote the number of symbols in a user's data packet. For user $(l,b)$ located in beam $b$ of cluster $l$, the transmitted symbol vector is $\mathbf{s}_{lb} = [s_{lb}(1), s_{lb}(2), \ldots, s_{lb}(M)]^T \in \mathbb{C}^{M\times 1}$. Each symbol $s_{lb}(m) \sim \mathcal{CN}(0,1)$ represents the data intended for user $(l,b)$ at time index $m$. These symbols are shaped using a pulse shaping filter $p(t)$, assumed to be a root-raised cosine (r.r.c.) pulse with roll-off factor $\beta$. The signal transmitted by gateway $l$, intended for user $(l,b)$, can be expressed as

$$\mathbf{x}_{l,lb}(t) = \sum_{m=1}^{M} \mathbf{w}_{lb} s_{lb}(m) p(t - mT_s), \tag{1}$$

where the vector $\mathbf{w}_{lb} \in \mathbb{C}^{B\times 1}$ is the precoding vector designed by gateway $l$ for user $(l,b)$, and $T_s$ represents the symbol duration. The received signal for user $(l,b)$ is given by

$$\begin{aligned} y_{lb}(t) = &\sum_{m=1}^{M} \mathbf{h}_{lb,l}\mathbf{w}_{lb} s_{lb}(m) p(t - mT_s - \boldsymbol{\tau}_{lb}^{l} T_s) \\ &+ \sum_{q\neq b}^{B}\sum_{m=1}^{M} \mathbf{h}_{lb,l}\mathbf{w}_{lq} s_{lq}(m) p(t - mT_s - \boldsymbol{\tau}_{lb}^{l} T_s) \\ &+ \sum_{j\neq l}^{L}\sum_{d=1}^{B}\sum_{m=1}^{M} \mathbf{h}_{lb,j}\mathbf{w}_{jd} s_{jd}(m) p(t - mT_s - \boldsymbol{\tau}_{lb}^{j} T_s) \\ &+ n_{lb}(t), \end{aligned} \tag{2}$$

here, $\mathbf{h}_{lb,j} \in \mathbb{C}^{1\times B}$ denotes the channel vector between user $(l,b)$ and gateway $j$, and $\boldsymbol{\tau}_{lb}^{j} = \boldsymbol{\tau}_{j,\text{sat}} + \boldsymbol{\tau}_{\text{sat},lb} \in [0,1)$ denotes the normalized time delay between gateway $j$ and user $(l,b)$ includes both gateway-to-satellite delay $\boldsymbol{\tau}_{j,\text{sat}}$ and satellite-to-user $\boldsymbol{\tau}_{\text{sat},lb}$ delay. Note that the system is synchronous when $\boldsymbol{\tau}_{lb}^{j} = 0$. In this expression, the first term is the desired signal. The second captures intra-cluster interference, which follows the same channel and arrives with identical delay, aligning with the desired signal. The third term represents inter-cluster interference, arriving with distinct timing delays $\tau_{lb}^{j}$ due to varying propagation paths. Finally, $n_{lb}(t)$ denotes the additive white Gaussian noise (AWGN) at user $(l,b)$. After reception, the signal $y_{lb}(t)$ is passed through a matched filter with an impulse response $p(t)$ and is sampled at time instants $t = nT_s + \boldsymbol{\tau}_{lb}^{l} T_s$, $n = 1, 2, \ldots, M$ yielding discrete-time signal as

$$\begin{aligned} y_{lb}(n) = &\mathbf{h}_{lb,l}\mathbf{w}_{lb} s_{lb}(n) + \sum_{q\neq b}^{B} \mathbf{h}_{lb,l}\mathbf{w}_{lq} s_{lq}(n) \\ &+ \sum_{j\neq l}^{L}\sum_{d=1}^{B}\sum_{m=1}^{M} \mathbf{h}_{lb,j}\mathbf{w}_{jd} s_{jd}(m) g[(m - n + \Delta\tau_{lb}^{(l,j)})T_s] \\ &+ n_{lb}(n), \end{aligned} \tag{3}$$

here, $\Delta\tau_{lb}^{(l,j)} = \boldsymbol{\tau}_{lb}^{l} - \boldsymbol{\tau}_{lb}^{j}$, $g(t) = p(t) * p(t)$, and $n_{lb}(n) = \int n_{lb}(t) p(t - (n + \boldsymbol{\tau}_{lb}^{l})T_s)\, dt$ denotes the filtered noise sample at the receiver. Finally, the received signal to interference plus noise ratio (SINR) at user $(l,b)$ can be calculated as

$$\text{SINR}_{lb} = \frac{\left|\mathbf{h}_{lb,l}\mathbf{w}_{lb}\right|^2}{\sum_{q\neq b}^{B}\left|\mathbf{h}_{lb,l}\mathbf{w}_{lq}\right|^2 + \sum_{j\neq l}^{L}\sum_{d=1}^{B} \eta_{lb}^{(l,j)}\left|\mathbf{h}_{lb,j}\mathbf{w}_{jd}\right|^2 + \sigma_{lb}^2}, \tag{4}$$

where, $\eta_{lb}^{(j,l)}$ represents the asynchronous factor associated with inter-cluster interference and can be calculated as in [9]

$$\eta_{lb}^{(l,j)} = 1 - \frac{\beta}{4} + \frac{\beta}{4}\cos\left(2\pi\Delta\tau_{lb}^{(l,j)}\right). \tag{5}$$

Since inter-cluster interference is misaligned with the desired signal, the matched filter samples it away from the pulse peak. Given the energy concentration of raised-cosine pulses at the symbol center, this reduces the captured power, reflected by an asynchronous factor $\eta_\tau < 1$. In contrast, intra-cluster interference is aligned, yielding $\eta_0 = 1$ with no power loss.

### B. Channel Model

The communication channel between satellite feeds and a user terminal is influenced by atmospheric propagation and the satellite beam's radiation pattern. For user $(l,b)$ served by gateway $l$, the channel coefficient is defined as

$$\mathbf{h}_{lb,l} = \tilde{\mathbf{g}} \odot \mathbf{B}_{lb,l}. \tag{6}$$

To include the rain attenuation effect, we adopt the latest model proposed in ITU-R[3] Recommendation P.618. The power gain is $\xi_{\text{dB}} = 20\log_{10}(\xi)$, where $\xi_{\text{dB}}$ follows lognormal distribution, i.e., $\ln(\xi_{\text{dB}}) \sim \mathcal{N}(\mu,\sigma)$ . Thus, the rain attenuation gain $\tilde{\mathbf{g}}$ from the feeds managed by $l$ gateway to user $(l,b)$ is given by

$$\tilde{\mathbf{g}} = \xi^{\frac{1}{2}} e^{-j\boldsymbol{\Phi}}, \tag{7}$$

where $\boldsymbol{\Phi} = \boldsymbol{\Phi}_1 + \boldsymbol{\Phi}_2$ is a phase vector, with $\boldsymbol{\Phi}_1 \sim \mathcal{U}(0, 2\pi)$ representing a uniformly distributed phase vector between feeds and the user, $\boldsymbol{\Phi}_2$ following a complex Gaussian distribution with zero mean and variance $\chi^2$ [11]. The channel gain $\mathbf{B}_{lb,l} \in \mathbb{C}^{1\times B}$, incorporating feed radiation pattern, path loss, receive antenna gain, and noise power, takes the form

$$\mathbf{B}_{lb,l} = \frac{G_R G_{lb,l}}{4\pi\frac{d_{lb,l}}{\lambda}\sqrt{\kappa T_R B}}\mathbf{1}_B, \tag{8}$$

here, $d_{lb,l}$, $\lambda$, and $\kappa$ denote the distance between user $(l,b)$ and feed, the carrier wavelength, Boltzmann constant, respectively. Parameters $T_R$, $B$, and $G_R$ represent the clear sky noise temperature of the receiver, the user link bandwidth, and the receiver antenna gain, respectively. Meanwhile, $\mathbf{1_B}$ is a $B$-dimensional all-one vector, and $G_{lb,l}$ is the multibeam antenna gain, which depends on the satellite transmitted antenna radiation pattern and the user location, and is given by

$$G_{lb,l} = G_{\max}\left(\frac{J_1(u_{lb,l})}{2u_{lb,l}} + 36\frac{J_3(u_{lb,l})}{u_{lb,l}^3}\right), \tag{9}$$

where $G_{\max}$ is the maximum beam gain at the beam center, $u_{lb,l} = 2.07123\sin\theta_{lb,l}/\sin\theta_{3\text{dB}}$ [12], $\theta_{lb,l}$ is the angle between the beam center and user $(l,b)$, $\theta_{3\text{dB}}$ is the 3 dB angle corresponding to the half power loss from the beam center, $J_1(\cdot)$ and $J_3(\cdot)$ are the first kind Bessel function of orders 1 and 3, respectively.

## III. Interference Alleviation

This section extends the system model by introducing intentional timing offsets to mitigate intra- and inter-cluster interference, and applies WMMSE precoding to maximize SE.

### A. Intentional Timing Offset for System Model

To further suppress interference, the satellite intentionally introduces different timing offsets between the transmitted signals for each user. As a result, both intra- and inter cluster interference becomes asynchronous with the desired signal. The resulting discrete-time signal for user $(l,b)$ after matched filtering and sampling at time $t = nT_s + \boldsymbol{\tau}_{lb}^l T_s$ is given by

$$\begin{aligned} y_{lb}(n) =& \mathbf{h}_{lb,l}\mathbf{w}_{lb}\mathbf{s}_{lb}(n) \\ &+ \sum_{q\neq b}^{B}\sum_{m=1}^{M}\mathbf{h}_{lb,l}\mathbf{w}_{lq}\mathbf{s}_{lq}(m)g[(m-n+\Delta\tau_{lb,lq}^l)T_s] \\ &+ \sum_{j\neq l}^{L}\sum_{d=1}^{B}\sum_{m=1}^{M}\mathbf{h}_{lb,j}\mathbf{w}_{jd}\mathbf{s}_{jd}(m)g[(m-n+\Delta\tau_{lb,jd}^{l,j})T_s] \\ &+ \boldsymbol{n}_{lb}(n), \end{aligned} \tag{10}$$

where $\Delta\tau_{lb,lq}^l = \boldsymbol{\tau}_{lb}^l - \boldsymbol{\tau}_{lq}^l$ , $\Delta\tau_{lb,jd}^{l,j} = \boldsymbol{\tau}_{lb}^l - \boldsymbol{\tau}_{jd}^j$ denote the timing delay differences for intra- and inter-cluster interference, respectively. The resulting SINR at user $(l,b)$ is given by

$$\text{SINR}_{lb} = \frac{|\mathbf{h}_{lb,l}\mathbf{w}_{lb}|^2}{a+b+\sigma_{lb}^2}, \tag{11}$$

where

$$a = \sum_{q\neq b}^{B}\eta_{bq}^{(l)}|\mathbf{h}_{lb,l}\mathbf{w}_{lq}|^2, b = \sum_{j\neq l}^{L}\sum_{d=1}^{B}\eta_{bd}^{(l,j)}|\mathbf{h}_{lb,j}\mathbf{w}_{jd}|^2.$$

In this formulation, the asynchronous factors $\eta_{bq}^{(l)}$ and $\eta_{bd}^{(l,j)}$ correspond to the intra- and inter-cluster interference, respectively. These factors can be expressed as

$$\eta_{bq}^{(l)} = 1 - \frac{\beta}{4} + \frac{\beta}{4}\cos\left(2\pi\Delta\tau_{lb,lq}^l\right). \tag{12}$$

$$\eta_{bd}^{(l,j)} = 1 - \frac{\beta}{4} + \frac{\beta}{4}\cos\left(2\pi\Delta\tau_{lb,jd}^{l,j}\right). \tag{13}$$

In this model, both $\eta_{bq}^{(l)}$ and $\eta_{bd}^{(l,j)}$ are less than one, indicating reduced intra- and inter-cluster interference and improved performance compared to natural asynchronous model.

### B. WMMSE Precoding for Asynchronous Transmission

Our goal is to maximize the sum rate across all users while satisfying per feed cluster transmit power constraints. The resulting optimization problem is formulated as

$$\begin{aligned} &\max_{\mathbf{W}}\sum_{l=1}^{L}\sum_{b=1}^{B}\log_2(1+\text{SINR}_{lb}) \\ &\text{s.t. }\sum_{b=1}^{B}\mathbf{Tr}(\mathbf{w}_{lb}\mathbf{w}_{lb}^H) \le P_l, \forall l\in\mathcal{L}, b\in\mathcal{B}, \end{aligned} \tag{14}$$

where the $\text{SINR}_{lb}$ is calculated according to (4) and (11) for natural and intentional asynchronous models, respectively. Additionally, $P_l$ denotes the total transmit power constraint for feed cluster $l$. Due to the non-convexity of the objective function, finding the global optimum is computationally challenging. To address this, we adopt the WMMSE method [13], which reformulates the problem into a more tractable weighted MSE minimization problem. The resulting optimization is defined as

$$\min_{\mathbf{W},\mathbf{v},\mathbf{c}}\sum_{l=1}^{L}\sum_{b=1}^{B}\left(v_{lb}\mathcal{E}_{lb} - \log v_{lb}\right), \tag{15}$$

where $\mathbf{c} = [c_{11}, c_{12}, \ldots, c_{LB}]$, $\mathbf{v} = [v_{11}, v_{12}, \ldots, v_{LB}]$, and $\mathbf{W} = [\mathbf{w}_{11}, \mathbf{w}_{12}, \ldots, \mathbf{w}_{LB}]$ represent the set of linear combiners, weights, and the corresponding precoding vectors of all users, respectively. Additionally, $\mathcal{E}_{lb}$ is mean-squared-error, which quantifies the difference between the estimated signal and the actual transmitted signal.

$$\mathcal{E}_{lb} = \mathbb{E}\left\{|\hat{s}_{lb} - s_{lb}|^2\right\} = 1 - 2\mathcal{R}\left\{c_{lb}\mathbf{h}_{lb,l}\mathbf{w}_{lb}\right\} + c_{lb}^* T_{lb} c_{lb}, \tag{16}$$

where $\hat{s}_{lb} = c_{lb}y_{lb}$ with $y_{lb}$ given by (3) and (10) for the natural and intentional asynchronous models, respectively. For simplicity, the time index $n$ is omitted throughout the analysis. The term $T_{lb}$ is given as

$$T_{lb} = \sum_{j=1}^{L}\sum_{d=1}^{B}\eta_\tau\,\mathbf{h}_{lb,j}\mathbf{w}_{jd}\mathbf{w}_{jd}^H\mathbf{h}_{lb,j}^H + \frac{\sum_{q=1}^{B}\text{Tr}(\mathbf{w}_{lq}\mathbf{w}_{lq}^H)}{P_l}\sigma_{lb}^2, \tag{17}$$

where the value of $\eta_\tau$ can be

$$\eta_\tau = \begin{cases} \text{Natural delay:} & \begin{cases} 1 & \text{if } l=j \text{ and } b\neq q, \\ \eta_{lb}^{(l,j)} & \text{if } j\neq l \end{cases} \\ \text{Intentional delay:} & \begin{cases} \eta_{bq}^{(l)} & \text{if } l=j \text{ and } b\neq q, \\ \eta_{bd}^{(l,j)} & \text{if } j\neq l \end{cases} \end{cases}. \tag{18}$$

In (15), the power constraint is incorporated directly into the objective function to simplify the precoder optimization, following [14]. The variables in the problem are tightly

coupled, making joint optimization intractable. To address this, we adopt a block coordinate descent (BCD) approach that iteratively updates one variable while keeping the others fixed. We define the optimization problem in (15) as follows

$$\mathcal{J} = \sum_{l=1}^{L}\sum_{b=1}^{B}\left(v_{lb}\mathcal{E}_{lb} - \log v_{lb}\right). \tag{19}$$

First, we update the linear combiner. Fixing $v_{lb}$ and $\mathbf{w}_{lb}$, we differentiate $\mathcal{J}$ with respect to $c_{lb}$ and set the result to zero

$$\begin{aligned}\frac{\partial \mathcal{J}}{\partial c_{lb}} = &\sum_{j=1}^{L}\sum_{d=1}^{B}\eta_\tau\, \mathbf{h}_{lb,j}\mathbf{w}_{jd}\mathbf{w}_{jd}^H\mathbf{h}_{lb,j}^H c_{lb} \\ &- \mathbf{h}_{lb,l}\mathbf{w}_{lb} + \frac{\sum_{q=1}^{B}\mathrm{Tr}\left(\mathbf{w}_{lq}\mathbf{w}_{lq}^H\right)}{P_l}\sigma_{lb}^2 c_{lb} = 0.\end{aligned} \tag{20}$$

This leads to the following update expression

$$c_{lb} = T_{lb}^{-1}\mathbf{h}_{lb,l}\mathbf{w}_{lb} \quad \forall l \in \mathcal{L},\, b \in \mathcal{B}. \tag{21}$$

Next, we update the weight. With $c_{lb}$ and $\mathbf{w}_{lb}$ fixed, the derivative of $\mathcal{J}$ with respect to $v_{lb}$, i.e., $\frac{\partial \mathcal{J}}{\partial v_{lb}} = 0$.

$$\frac{\partial \mathcal{J}}{\partial v_{lb}} = \mathcal{E}_{lb} - v_{lb}^{-1} = 0. \tag{22}$$

Substituting the optimal linear combiner back into (16), the updated weight becomes

$$v_{lb} = \mathcal{E}_{lb}^{-1} = \left(1 - T_{lb}^{-1}\left|\mathbf{h}_{lb,l}\mathbf{w}_{lb}\right|^2\right)^{-1} \quad \forall l \in \mathcal{L},\, b \in \mathcal{B}. \tag{23}$$

Finally, we update the precoder. keeping $c_{lb}$ and $v_{lb}$ fixed, and setting $\frac{\partial \mathcal{J}}{\partial \mathbf{w}_{lb}} = 0$.

$$\begin{aligned}\frac{\partial \mathcal{J}}{\partial \mathbf{w}_{lb}} = &\sum_{j=1}^{L}\sum_{d=1}^{B}\eta_\tau \mathbf{h}_{jd,l}^H c_{jd} v_{jd} c_{jd}^* \mathbf{h}_{jd,l}\mathbf{w}_{lb} \\ &- c_{lb}v_{lb}\mathbf{h}_{lb,l}^H + \frac{\sum_{q=1}^{B}\sigma_{lq}^2 c_{lq}v_{lq}c_{lq}^*\mathbf{w}_{lb}}{P_l} = 0.\end{aligned} \tag{24}$$

Solving this gives the update of the precoding vector

$$\mathbf{w}_{lb} = \mathbf{Q}^{-1}c_{lb}v_{lb}\mathbf{h}_{lb,l}^H \quad \forall l \in \mathcal{L},\, b \in \mathcal{B}, \tag{25}$$

where $\mathbf{Q}$ is given as

$$\mathbf{Q} = \sum_{j=1}^{L}\sum_{d=1}^{B}\eta_\tau \mathbf{h}_{jd,l}^H c_{jd}v_{jd}c_{jd}^*\mathbf{h}_{jd,l} + \left(\frac{\sum_{q=1}^{B}\sigma_{lq}^2 c_{lq}v_{lq}c_{lq}^*}{P_l}\right)\mathbf{I}. \tag{26}$$

From (21), (23), and (25), $c_{lb}$,$v_{lb}$, and $\mathbf{w}_{lb}$ are computed alternately until convergence to a local optimum. The detailed iterative process is illustrated in **Algorithm 1**.

## IV. Numerical Simulations and Results

This section evaluates SE under three models: synchronous, natural asynchrony, and intentional asynchrony. The simulated system consists of 5 gateways, each managing 7 beams. The topology is shown in Fig.2, with parameters listed in Table 1.

Fig. 3 compares the SE across three transmission models using different precoders: WMMSE, minimum-mean-square-error (MMSE), and maximum ratio transmission (MRT). The

**Algorithm 1** Propose WMMSE Precoding for Solving (19)

**Require:** Channel matrix $\mathbf{h}_{lb,l}$, delay $\boldsymbol{\tau}_{lb}^{l}$, total power budget $P_l$, $\forall l \in \mathcal{L}, b \in \mathcal{B}$; compute $\eta_{lb}^{(l,j)}$ (natural asynchronous model, Eq. (6)), $\eta_{bq}^{(l)}$, $\eta_{bd}^{(l,j)}$ (intentional asynchronous model, Eq. (10)and (11) respectively),

**Ensure:** Precoding vector $\mathbf{w}_{lb}$, initialized via ZF, satisfying:

$$\sum_{q=1}^{\mathcal{B}}\mathrm{Tr}(\mathbf{w}_{lq}\mathbf{w}_{lq}^H) \le P_l, \quad \forall l \in \mathcal{L}$$

1: **repeat**
2: Compute the linear combiners $c_{lb}$, $\forall l \in \mathcal{L}, b \in \mathcal{B}$ (Eq. (21),
3: Compute the weights $v_{lb}$, $\forall l \in \mathcal{L}, b \in \mathcal{B}$ (Eq. (23)),
4: Update the precoder $\mathbf{w}_{lb}$, $\forall l \in \mathcal{L}, b \in \mathcal{B}$ (Eq. (25)),
5: **until** convergence or max iterations.

TABLE I
SIMULATION PARAMETERS

| Parameter | Value |
|---|---|
| Center frequency | 20 GHz |
| Beam radius | 100 km |
| Rain fading mean | -2.6 dB |
| Rain fading variance | 1.63 dB |
| Maximum antenna transmit gain | 52 dBi |
| 3 dB angle | $\theta_{3\text{dB}} = 0.4^\circ$ |
| Receiver antenna gain | 41.7 dBi |
| User Link Bandwidth | 500 MHz |
| Free space loss | 210 dB |
| Clear sky receiver temperature | 207 K |
| Boltzmann constant | $1.380649 \times 10^{-23}$ J/K |
| Number of gateways | $L$ = 5 |
| Number of beams per gateway | B = 7 |
| Roll-off factor | $\beta$=0.8 |

MRT precoder is given by $\mathbf{w}_{l,lb} = \mathbf{h}_{l,lb}$, scaled to satisfy the per-gateway power constraint. Overall, asynchronous transmission consistently outperforms the synchronous model, which suffers from higher interference due to the assumed signal alignment. Between the two asynchronous models, intentional asynchrony achieves the highest SE by mitigating both intra- and inter-cluster interference, while natural asynchrony mainly addresses inter-cluster interference. At 10 dB, WMMSE under natural and intentional asynchrony yields SE gains of approximately 0.64% and 9.94%, respectively, compared to the synchronous case. Additionally, WMMSE outperforms MMSE and MRT in all scenarios, confirming its superiority in interference mitigation and throughput enhancement.

Fig. 4 presents the SE of WMMSE precoding using both root-raised cosine (r.r.c.) and rectangular (rect) pulse shaping. For the rect pulse, the asynchronous factor is given by [9] $\eta_{\text{rect}} = \Delta\tau^2 + (1-\Delta\tau)^2$. It is observed that asynchronous transmission consistently outperforms the conventional synchronous, with intentional asynchrony achieving the highest SE across all SNRs. Additionally, rect pulses outperform r.r.c. due to their strictly time-limited nature, leading to lower asynchronous factors and better interference suppression.

Fig. 5 shows the impact of the roll-off factor $\beta$ on SE under synchronous and asynchronous transmission. At $\beta = 0$, corresponding to zero-excess bandwidth pulse, $\eta_\tau = 1$, and the SE of asynchronous and synchronous transmission is identical, yielding no performance gain. As $\beta$ increases, $\eta_\tau$ decreases,

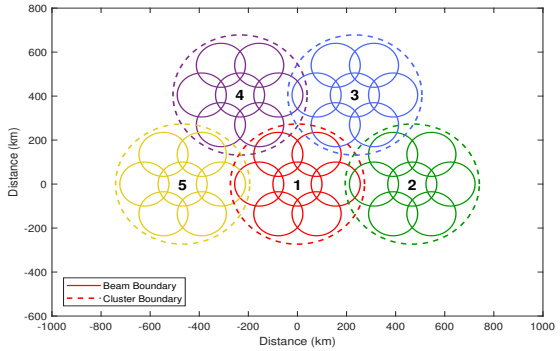


Fig. 2. Beam pattern with five clusters, each consisting of seven beams.

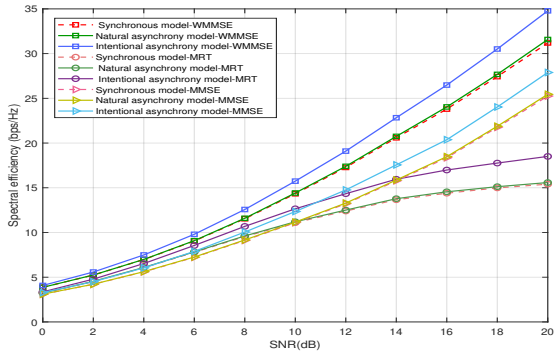


Fig. 3. Spectral efficiency of various schemes versus SNR.

enhancing interference suppression and improving SE.

## V. Conclusion

This paper investigated time asynchrony in multigateway multibeam satellite systems as a means to improve interference mitigation and system performance. Both natural asynchrony, arising from gateway spacing, and intentional asynchrony, implemented via per-user timing offsets at the satellite, were analyzed, and applied a WMMSE precoder to suppress the resulting interference. Simulation results show that natural asynchrony boosts spectral efficiency by 0.64%, while intentional asynchrony delivers a 9.94% gain at 10 dB. These results confirm that time asynchrony, when properly utilized, can significantly enhance future multigateway satellite systems.

## VI. Acknowledgement

This work was supported in part by the National Natural Science Foundation of China under Grant 62271376, and in part by the Guangdong Natural Science Fund for Distinguished Young Scholar under Grant 2023B1515020079.

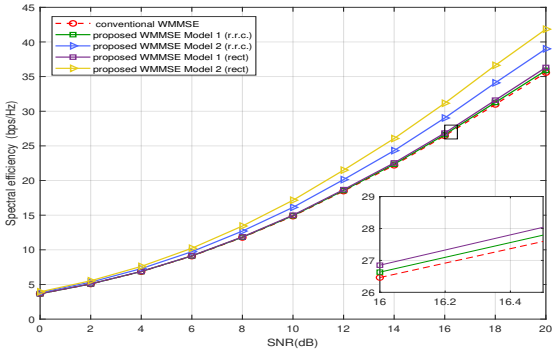


Fig. 4. Spectral efficiency of various WMMSE models versus SNR.

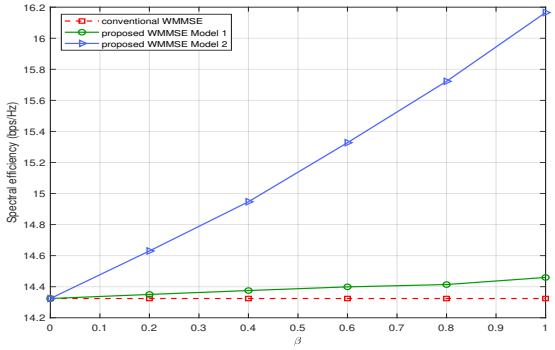


Fig. 5. Spectral efficiency versus roll-off factor $\beta$ with SNR = 10dB.

## References

[1] M. Khammassi, A. Kammoun, and M.-S. Alouini, "Precoding for high-throughput satellite communication systems: A survey," *IEEE Commun. Surv. & Tuto.*, vol. 26, no. 1, pp. 80–118, 2024.

[2] R. De Gaudenzi, P. Angeletti, D. Petrolati, and E. Re, "Future technologies for very high throughput satellite systems," *Int. J. Satell. Commun. Netw.*, vol. 38, no. 2, pp. 141 – 161, 2020.

[3] I. Ahmad, K. D. Nguyen, N. Letzepis, G. Lechner, and V. Joroughi, "Zero-forcing precoding with partial csi in multibeam high throughput satellite systems," *IEEE Trans. Veh. Technol.*, vol. 70, no. 2, pp. 1410–1420, 2021.

[4] V. Joroughi, M. A. Vázquez, and A. I. Pérez-Neira, "Precoding in multigateway multibeam satellite systems," *IEEE Trans. Wireless Commun.*, vol. 15, no. 7, pp. 4944–4956, 2016.

[5] J. Wang, L. Zhou, K. Yang, X. Wang, and Y. Liu, "Multicast precoding for multigateway multibeam satellite systems with feeder link interference," *IEEE Trans. Wireless Commun.*, vol. 18, no. 3, pp. 1637–1650, 2019.

[6] H. Ali, Y. He, X. Feng, K. Liu, M. Chen, Q. Su, and R. Chen, "Multigateway hybrid space-ground precoding for multi-beam satellite communications," in *Int. Conf. Commun. Signal Process. Appl. (ICCSPA)*, 2024, pp. 1–5.

[7] Q. Su, X. Feng, and R. Chen, "Multigateway robust precoding for multibeam satellite systems with feeder link interference," in *2024 IEEE 99th Veh. Technol. Conf. (VTC2024-Spring)*, 2024, pp. 1–6.

[8] H. Zhang, N. B. Mehta, A. F. Molisch, J. Zhang, and S. H. Dai, "Asynchronous interference mitigation in cooperative base station systems," *IEEE Trans. Wireless Commun.*, vol. 7, no. 1, pp. 155–165, 2008.

[9] M. Ganji, X. Zou, and H. Jafarkhani, "Exploiting time asynchrony in multi-user transmit beamforming," *IEEE Trans. Wireless Commun.*, vol. 19, no. 5, pp. 3156–3169, 2020.

[10] X. Chen and Z. Luo, "Asynchronous interference mitigation for leo multi-satellite cooperative systems," *IEEE Trans. Wireless Commun.*, vol. 23, no. 10, pp. 14 956–14 971, 2024.

[11] V. Joroughi, M. A. Vázquez, and A. I. Pérez-Neira, "Generalized multicast multibeam precoding for satellite communications," *IEEE Trans. Wireless Commun.*, vol. 16, no. 2, pp. 952–966, 2016.

[12] G. Zheng, S. Chatzinotas, and B. Ottersten, "Generic optimization of linear precoding in multibeam satellite systems," *IEEE Trans. Wireless Commun.*, vol. 11, no. 6, pp. 2308–2320, 2012.

[13] Q. Shi, M. Razaviyayn, Z.-Q. Luo, and C. He, "An iteratively weighted mmse approach to distributed sum-utility maximization for a mimo interfering broadcast channel," *IEEE Trans. Signal Process.*, vol. 59, no. 9, pp. 4331–4340, 2011.

[14] Q. Hu, Y. Cai, Q. Shi, K. Xu, G. Yu, and Z. Ding, "Iterative algorithm induced deep-unfolding neural networks: Precoding design for multiuser mimo systems," *IEEE Trans. Wireless Commun.*, vol. 20, no. 2, pp. 1394–1410, 2021.